

Bias in Dobson total ozone measurements at high latitudes due to approximations in calculations of ozone absorption coefficients and air mass

G. Bernhard,¹ R. D. Evans,² G. J. Labow,³ and S. J. Oltmans²

Received 29 October 2004; revised 14 January 2005; accepted 10 February 2005; published 20 May 2005.

[1] The Dobson spectrophotometer is the primary standard instrument for ground-based measurements of total column ozone. The accuracy of its data depends on the knowledge of ozone absorption coefficients used for data reduction. We document an error in the calculations that led to the set of absorption coefficients currently recommended by the World Meteorological Organisation (WMO). This error has little effect because an empirical adjustment was applied to the original calculations before the coefficients were adopted by WMO. We provide evidence that this adjustment was physically sound. The coefficients recommended by WMO are applied in the Dobson network without correction for the temperature dependence of the ozone absorption cross sections. On the basis of data measured by Dobson numbers 80 and 82, which were operated by the National Oceanic and Atmospheric Administration (NOAA) Climate Monitoring and Diagnostics Laboratory at the South Pole, we find that omission of temperature corrections may lead to systematic errors in Dobson ozone data of up to 4%. The standard Dobson ozone retrieval method further assumes that the ozone layer is located at a fixed height. This approximation leads to errors in air mass calculations, which are particularly relevant at high latitudes where ozone measurements are performed at large solar zenith angles (SZA). At the South Pole, systematic errors caused by this approximation may exceed 2% for SZAs larger than 80°. The bias is largest when the vertical ozone distribution is distorted by the “ozone hole” and may lead to underestimation of total ozone by 4% at SZA = 85° (air mass 9). Dobson measurements at the South Pole were compared with ozone data from a collocated SUV-100 UV spectroradiometer and Version 8 overpass data from NASA’s Total Ozone Mapping Spectrometer (TOMS). Uncorrected Dobson ozone values tend to be lower than data from the two other instruments when total ozone is below 170 Dobson units or SZAs are larger than 80°. When Dobson measurements are corrected for the temperature dependence of the ozone absorption cross section and accurate air mass calculations are implemented, data from the three instruments agree with each other to within ±2% on average and show no significant dependence on SZA or total ozone.

Citation: Bernhard, G., R. D. Evans, G. J. Labow, and S. J. Oltmans (2005), Bias in Dobson total ozone measurements at high latitudes due to approximations in calculations of ozone absorption coefficients and air mass, *J. Geophys. Res.*, *110*, D10305, doi:10.1029/2004JD005559.

1. Introduction

[2] The Dobson spectrophotometer was developed by G. M. B. Dobson in the 1920s [*Dobson and Harrison*, 1926; *Dobson*, 1931] and is still the standard instrument for measuring the atmospheric total ozone column. Climate Monitoring and Diagnostics Laboratory (CMDL) maintains 15 instruments, and operates the World Dobson Ozone Calibration Centre under the auspices of WMO’s Global

Atmosphere Watch program. There are about 100 Dobson instruments in operation worldwide. A list of stations can be found on the website <http://www.chmi.cz/meteo/ozon/dobsonweb/stations.htm>. Total ozone can be calculated from direct Sun or zenith sky observations. Here we discuss direct Sun measurements only.

[3] The Dobson instrument, its measurement errors, and calibration procedures have been described in several publications [e.g., *Komhyr*, 1980a; *Basher*, 1982; *Komhyr et al.*, 1989]. Measurement errors typically increase under low-Sun conditions. For example, direct Sun measurements are always contaminated to some degree by diffuse radiation scattered by air molecules into the Dobson’s field of view. As the Sun sets, the relative contribution of diffuse radiation increases. This can result in an apparent decrease in ozone, since diffuse radiation is less attenuated by ozone than

¹Biospherical Instruments, Inc., San Diego, California, USA.

²Climate Monitoring and Diagnostics Laboratory, NOAA, Boulder, Colorado, USA.

³NASA Goddard Space Flight Center, Greenbelt, Maryland, USA.

direct radiation at short wavelengths and large SZAs [Josefsson, 1992; Nichol and Valenti, 1993]. At low Sun, errors can also arise due to light scattering within the Dobson instrument [Komhyr, 1980b].

[4] In this paper, we focus on two additional sources of error: (1) the effects of temperature and vertical ozone distribution (i.e., the ozone profile) on the values of ozone absorption coefficients used to calculate total ozone from Dobson raw data and (2) systematic errors due to approximations in air mass calculations. Error source 1 is relevant at all locations and is well recognized. For example, Komhyr *et al.* [1993] calculated ozone absorption coefficients using 46 combinations of 11 temperature profiles and 22 ozone profiles. The resulting values of the absorption coefficient for Dobson AD-pair measurements varied between 1.3971 and 1.4664; the standard deviation of the 46 different values was 0.016. Brinkma *et al.* [2000] studied the effect of the annual cycle of the temperature profile on Dobson AD-pair measurements at Lauder, New Zealand (45°S, 170°E). They found systematic errors in Dobson results with an amplitude of 2% if the effect of temperature on the absorption cross section is not corrected. Van Roozendaal *et al.* [1998] performed a similar analysis for Arosa, Switzerland (46°N, 9°E), and found that the seasonal change in the atmospheric temperature accounts for a seasonal variation of uncorrected Dobson data with an amplitude of 0.9% and a systematic offset of approximately 1%. All previous calculations did not consider latitudes larger than 75°. Cooler stratospheric temperatures at high latitudes could lead to larger systematic errors. Error source 2 becomes important when ozone measurements are performed at large SZAs, a common occurrence at high latitudes.

2. Theoretical Background

2.1. Measurement Equation

[5] According to Beer-Lambert's law, spectral irradiance $E(\lambda)$ from the direct solar beam at the Earth's surface is calculated:

$$E(\lambda) = E_0(\lambda) 10^{-\alpha(\lambda)X\mu - \beta(\lambda)\frac{p_S}{p_0}m_R - \delta(\lambda)m_a} \quad (1)$$

where

- $E(\lambda)$ direct normal irradiance at the surface at wavelength λ ;
- $E_0(\lambda)$ extraterrestrial irradiance at wavelength λ ;
- $\alpha(\lambda)$ monochromatic ozone absorption coefficient (base 10) at wavelength λ (calculations are presented on the basis of "base 10" rather than "base e " to better compare with historic data);
- X total column ozone;
- μ relative optical air mass corresponding to ozone absorption (see section 2.3 for definition of relative optical air mass);
- $\beta(\lambda)$ Rayleigh optical depth (base 10) at 1013.25 hPa;
 - p_S station pressure;
 - p_0 mean sea level pressure (1013.25 hPa);
 - m_R relative optical air mass corresponding to Rayleigh scattering (extinction);
- $\delta(\lambda)$ aerosol optical depth (base 10) at wavelength λ ;
- m_a relative optical air mass corresponding to aerosol scattering (extinction).

[6] The Dobson spectrophotometer does not measure irradiance at a single wavelength but instead determines the difference between irradiance at two wavelengths, one strongly and the other weakly affected by ozone absorption. Several wavelength pairs are used in Dobson spectrometry (Table 1). The expression for calculating total ozone using wavelength pair observations is obtained by evaluating equation (1) for two different wavelengths, λ and λ' with $\lambda < \lambda'$. By taking the logarithm of the two equations associated with λ and λ' and calculating their difference, the following expression for the total column ozone X is derived [Komhyr, 1980b; Basher, 1982]:

$$X = \frac{N - [\beta(\lambda) - \beta(\lambda')]\frac{p_S}{p_0}m_R - [\delta(\lambda) - \delta(\lambda')]m_a}{[\alpha(\lambda) - \alpha(\lambda')]\mu}, \quad (2)$$

where $N = \log[E_0(\lambda)/E_0(\lambda')] - \log[E(\lambda)/E(\lambda')]$.

[7] Since the aerosol optical depth is usually not well known, ozone retrievals with the standard Dobson method are based on a combination of two wavelength-pair measurements. For example, when the A and D wavelength pairs (Table 1) are used, X is calculated with

$$X = \frac{N_A - N_D - \Delta\beta_{AD}\frac{p_S}{p_0}m_R - \Delta\delta_{AD}m_a}{\Delta\alpha_{AD}\mu} \quad (3)$$

where

$$\begin{aligned} N_A &= \log[E_0(305.5)/E_0(325)] - \log[E(305.5)/E(325)], \\ N_D &= \log[E_0(317.5)/E_0(339.9)] - \log[E(317.5)/E(339.9)], \\ \Delta\alpha_{AD} &= [\alpha(305.5) - \alpha(325)] - [\alpha(317.5) - \alpha(339.9)], \\ \Delta\beta_{AD} &= [\beta(305.5) - \beta(325)] - [\beta(317.5) - \beta(339.9)], \\ \Delta\delta_{AD} &= [\delta(305.5) - \delta(325)] - [\delta(317.5) - \delta(339.9)], \end{aligned}$$

and wavelength arguments are given in nm. Total ozone can also be calculated from other wavelength double pairs, such as the CD pair, by modifying equation (3) accordingly [Basher, 1982].

[8] Using the "double-pair technique" mostly eliminates the effect of aerosols on ozone retrievals [Basher, 1982]. This is particularly the case at high southern latitudes where aerosol concentrations are low. Aerosol optical depth $\delta(\lambda)$ can be approximated with Ångström's turbidity formula $\delta(\lambda) = (b/\ln(10))(\lambda/1000)^{-a}$, where λ is wavelength in nm. During periods with background aerosol conditions at the South Pole, the coefficients a and b are approximately 1.5 and 0.007, respectively [Climate Monitoring and Diagnostics Laboratory (CMDL), 2004, Figure 3.32], leading to $\Delta\delta_{AD} = -0.00006$ and $\Delta\delta_{CD} = -0.00003$. Although $\Delta\delta_{AD}$ can be as high as -0.001 during periods affected by volcanic aerosols, the value is still very small compared to the term for ozone absorption ($\Delta\alpha_{AD} = 1.432$). The effect of aerosols is therefore ignored in the following calculations.

2.2. Calculation of Effective Ozone Absorption Coefficients $\bar{\alpha}_i$

[9] The absorption coefficients $\alpha(\lambda)$ are calculated from the ozone absorption cross section $\sigma(\lambda, T)$ and the altitude-dependent ozone number density $\rho(z)$:

$$\alpha(\lambda) = \frac{1}{X} \int_{z_0}^{\infty} \sigma(\lambda, T(z))\rho(z)dz, \quad (4)$$

Table 1. Dobson Wavelengths, Slit Function Parameters, and Absorption Coefficients

Wavelength, nm or pair	Slit Function ^a			Effective Ozone Absorption Coefficient, ^c (atm cm) ⁻¹				
	Base, nm	FWHM, nm	Top, nm	<i>Komhyr et al.</i> [1993] ^b			Our Calculation	
				$\overline{\alpha}_i^{\text{approx}}$	$\overline{\alpha}_i$	$\overline{\alpha}_i^{\text{adjusted}}$	$\overline{\alpha}_i^{\text{approx}}$	$\overline{\alpha}_i$
305.5	1.86	1.01	0.16	1.917	1.915		1.915	1.914
325.0	5.00	3.56	1.06	0.115	0.109		0.115	0.110
A				1.802	1.806	1.806	1.800	1.805
308.9	1.86	1.02	0.18	1.244	1.239		1.241	1.242
329.1	5.32	3.50	1.68	0.065	0.062		0.065	0.063
B				1.179	1.177	1.192	1.176	1.180
311.5	1.94	1.06	0.18	0.870	0.873		0.868	0.871
332.4	5.94	3.71	1.48	0.039	0.040		0.040	0.039
C				0.831	0.833	0.833	0.828	0.832
317.5	2.12	1.20	0.28	0.379	0.384		0.384	0.387
339.9	6.88	4.20	1.52	0.010	0.017		0.010	0.010
D				0.369	0.367	0.374	0.373	0.377
AD				1.433	1.439	1.432	1.427	1.428
BD				0.811	0.810	0.818	0.803	0.803
CD				0.462	0.466	0.459	0.455	0.455

^aSlit function parameters Base, FWHM, and Top define full width wavelength range at base, half maximum, and top, respectively, of trapezoidal slit functions fitted to plots in Figure 1 of *Komhyr et al.* [1993].

^bEffective ozone absorption coefficient $\overline{\alpha}_i^{\text{approx}}$, $\overline{\alpha}_i$, and $\overline{\alpha}_i^{\text{adjusted}}$ were taken from Tables 6a, 11, and 13 of *Komhyr et al.* [1993], respectively. Coefficient $\overline{\alpha}_i^{\text{approx}}$ was adjusted to describe absorption at -46.3°C rather than -45°C .

^cEffective ozone absorption coefficients are given in units of (atm cm)⁻¹ to ease comparisons with historic data; 1 atm cm equals 1000 Dobson units or 2.69×10^{19} molecules per cm².

where z_0 is station elevation and T is temperature in Kelvin. Equation (4) implies that $\alpha(\lambda)$ depends on the atmospheric ozone and temperature distribution. The ozone column X is calculated by integrating over the ozone profile:

$$X = \frac{kT_0}{p_0} \int_{z_0}^{\infty} \rho(z) dz, \quad (5)$$

where T_0 is 273.15 K and k is the Boltzmann constant.

[10] The *Bass and Paur* [1985] ozone absorption cross sections (O_3CS) are implemented throughout this paper for wavelengths below 339.982 nm. Above 340 nm, where Bass and Paur data are not available, the *Molina and Molina* [1986] O_3CS was used. Cross sections were multiplied with the correction factor

$$f_C = 1.0112 - 0.6903/[87.3 - (T - T_0)] \quad (6)$$

as suggested by *Komhyr et al.* [1993] based on results by *Barnes and Mauersberger* [1987]. This factor corrects for a temperature dependence of the O_3CS at 253.7 nm, which was not considered by *Bass and Paur* [1985]. The *Bass and Paur* [1985] O_3CS with the *Barnes and Mauersberger* [1987] correction is also implemented by the Dobson network. A comparison of the *Bass and Paur* [1985] O_3CS with more recent measurements of the O_3CS has been compiled by *Orphal* [2003].

[11] Equations (1)–(3) are only applicable to monochromatic radiation. Owing to the finite bandwidth of the Dobson, $\alpha(\lambda)$ has to be replaced in equations (1)–(3) by the effective ozone absorption coefficient $\overline{\alpha}_i$, which is a weighted average of $\alpha(\lambda)$ [*Basher*, 1982]:

$$\overline{\alpha}_i = \frac{-1}{X_{\mu}} \log \left(\frac{\int E_0(\lambda) S(\lambda, \lambda_i) 10^{-\alpha(\lambda) X_{\mu} - \beta(\lambda) \frac{p_0}{p_0} m_R} d\lambda}{\int E_0(\lambda) S(\lambda, \lambda_i) 10^{-\beta(\lambda) \frac{p_0}{p_0} m_R} d\lambda} \right), \quad (7)$$

where $S(\lambda, \lambda_i)$ is the Dobson slit function for nominal wavelength λ_i .

[12] For consistency checks, we also consider the approximated (or slit function weighted) effective ozone absorption coefficient $\overline{\alpha}_i^{\text{approx}}$ defined as

$$\overline{\alpha}_i^{\text{approx}} = \frac{\int \alpha(\lambda) S(\lambda, \lambda_i) d\lambda}{\int S(\lambda, \lambda_i) d\lambda}. \quad (8)$$

2.3. Calculation of Air Mass

[13] Relative optical air mass m is defined as the ratio of the actual (slant) optical path length taken by the direct solar beam to the analogous vertical path when the Sun is overhead from the surface to the top of the atmosphere. It can be expressed by [*Thomason et al.*, 1983]:

$$m(\theta_0, \lambda) = \frac{1}{\int_{z_0}^{\infty} \sigma(\lambda, T(z)) \rho(z) dz} \int_{z_0}^{\infty} \frac{\sigma(\lambda, T(z)) \rho(z) dz}{\left[1 - \left(\frac{n_0 z_0 \sin(\theta_0)}{n(z) z} \right)^2 \right]^{0.5}}, \quad (9)$$

where $n(z)$ is the index of refraction of air as a function of altitude z , $n_0 = n(z_0)$, and θ_0 is the apparent SZA at which the Sun appears at the Earth's surface. Owing to refraction, θ_0 is smaller than the true SZA, θ , at which the Sun would appear if the Earth had no atmosphere. The dependence of $m(\theta_0, \lambda)$ on λ is negligible in the wavelength range considered here. All air mass calculations in this paper are based on $\lambda = 310$ nm. If the attenuating layer is a delta function at height h above sea level, equation (9) can be simplified to

$$m(\theta_0) = \frac{n_h(R+h)}{\left[n_h^2(R+h)^2 - n_0^2(R+r)^2 \sin^2 \theta_0 \right]^{0.5}}, \quad (10)$$

Table 2. Parameters for Calculation of $\bar{\alpha}_i$ for Standard Conditions

Parameter	Our Implementation	<i>Komhyr et al.</i> [1993]
Atmosphere profile	1986 U.S. standard atmosphere [<i>Anderson et al.</i> , 1986]	1962 U.S. standard atmosphere
Effective temperature T_{eff}	-46.4°C	-46.3°C
Ozone profile	<i>Bhartia et al.</i> [1985] for 45°N and 325 DU	<i>Bhartia et al.</i> [1985] for 45°N and 325 DU
Air mass	2	2
Ozone absorption cross section	<i>Bass and Paur</i> [1985], adjusted with <i>Barnes and Mauersberger</i> [1987] ^a	<i>Bass and Paur</i> [1985], adjusted with <i>Barnes and Mauersberger</i> [1987] ^a
Slit functions	trapezoidal fits to Figure 1 of <i>Komhyr et al.</i> [1993]	Figure 1 of <i>Komhyr et al.</i> [1993]
Extraterrestrial spectrum	<i>Gueymard</i> [2004] ^b	<i>Furukawa et al.</i> [1967]
Rayleigh optical depth	equation (30) of <i>Bodhaine et al.</i> [1999]	<i>Bates</i> [1984]

^aIn our implementation the *Molina and Molina* [1986] O₃CS was used to extend the *Bass and Paur* [1985] O₃CS to wavelengths beyond 340 nm; *Komhyr et al.* [1993] used unpublished data by A. M. Bass and R. J. Paur.

^bThe extraterrestrial spectrum (ETS) by *Gueymard* [2004] has a comparatively coarse resolution. We therefore superimposed the fine structure of the high-resolution “Kitt Peak solar flux atlas” [*Kurucz et al.*, 1984] (see ftp://ftp.noaa.edu/fts/fluxatl/). The composite spectrum is identical with the spectrum labeled $E_{\text{Gueymard}}(\lambda)$ presented in the work by *Bernhard et al.* [2004]. This publication also discusses the construction and accuracy of the spectrum.

where R is the radius of the Earth, r is altitude of the station, and n_h is the refractive index at height h . The standard Dobson method [*Basher*, 1982] assumes that the ozone layer is located at height h and that $n_0 = n_h = 1$. In this case, the relative air mass attributed to ozone absorption becomes

$$\mu^{\text{approx}}(\theta_0) = \frac{R+h}{\left[(R+h)^2 - (R+r)^2 \sin^2 \theta_0\right]^{0.5}}. \quad (11)$$

3. Validation of $\bar{\alpha}_i$ Calculation for Standard Ozone Profile

[14] *Komhyr et al.* [1993] (denoted as K93 hereinafter) calculated a set of ozone absorption coefficients $\bar{\alpha}_i$ for a “standard” ozone profile. These calculations form the basis of the set of coefficients currently implemented by CMDL and WMO’s Dobson network [*Hudson et al.*, 1991]. To validate the calculations by K93, we determined $\bar{\alpha}_i$ with similar input parameters as used by K93, and compared the results. Parameters of the two implementations are given in Table 2.

[15] Since numerical data of the slit functions used by K93 were not available, we fitted symmetrical trapezoids centered at the nominal Dobson wavelengths to the experimentally determined slit functions of Dobson instrument number 83 plotted in Figure 1 of K93. Top and base widths of these trapezoids are given in Table 1.

[16] When K93 applied their set of “standard” coefficients $\bar{\alpha}_i$ to observations made by the World Standard Dobson Spectrophotometer number 83 at Mauna Loa observatory, they found differences in calculated total ozone values of up to 3.8% depending on the choice of Dobson wavelength pairs. To lessen these discrepancies, $\bar{\alpha}_B$ and $\bar{\alpha}_D$ were empirically increased by 1.3% and 2.0%, respectively. The adjusted set of coefficients (labeled $\bar{\alpha}_i^{\text{adjusted}}$ in the following) was recommended by the International Ozone Commission (IOC) to be used for data archived in the World Ozone and Ultraviolet Radiation Data Centre (WOUDC), and adopted by WMO on 1 January 1992 [*Hudson et al.*,

1991]. The adjusted set of coefficients is also the set currently implemented by CMDL.

[17] Figure 1 shows our calculation of the monochromatic ozone absorption coefficient $\alpha(\lambda)$ and the associated effective

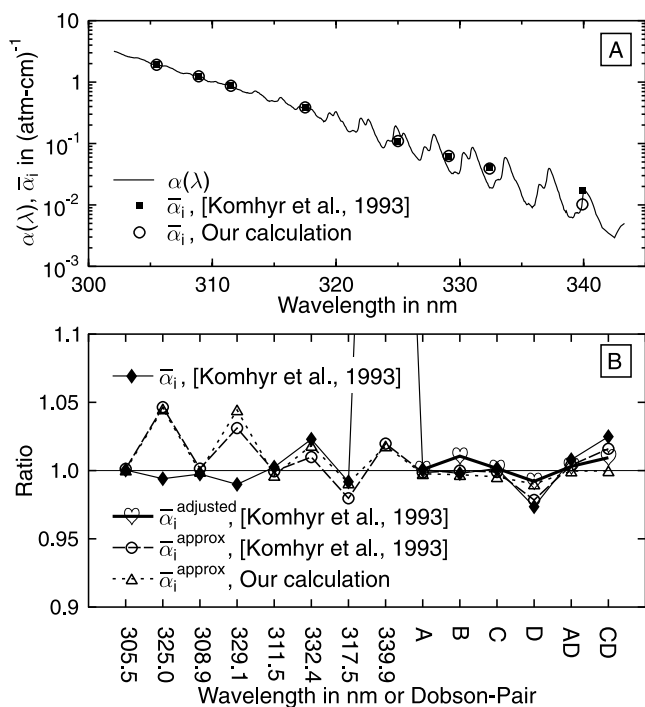


Figure 1. Comparison of monochromatic ozone absorption coefficient $\alpha(\lambda)$ and associated effective ozone absorption coefficients $\bar{\alpha}_i$, $\bar{\alpha}_i^{\text{approx}}$, and $\bar{\alpha}_i^{\text{adjusted}}$, calculated by *Komhyr et al.* [1993] and us for “standard” conditions defined in Table 2. (a) The coefficients $\alpha(\lambda)$ and $\bar{\alpha}_i$, calculated by *Komhyr et al.* [1993] and us. (b) Ratio of $\bar{\alpha}_i$, $\bar{\alpha}_i^{\text{adjusted}}$, and $\bar{\alpha}_i^{\text{approx}}$ as calculated by *Komhyr et al.* [1993] to $\bar{\alpha}_i$ calculated by us. The ratio of our calculations of $\bar{\alpha}_i^{\text{approx}}$ to our calculation of $\bar{\alpha}_i$ is also shown. The ratio of *Komhyr*’s and our calculation of $\bar{\alpha}_{339.9}$ is 1.67 and off the chart. Lines are only given for easier identification of the different data sets.

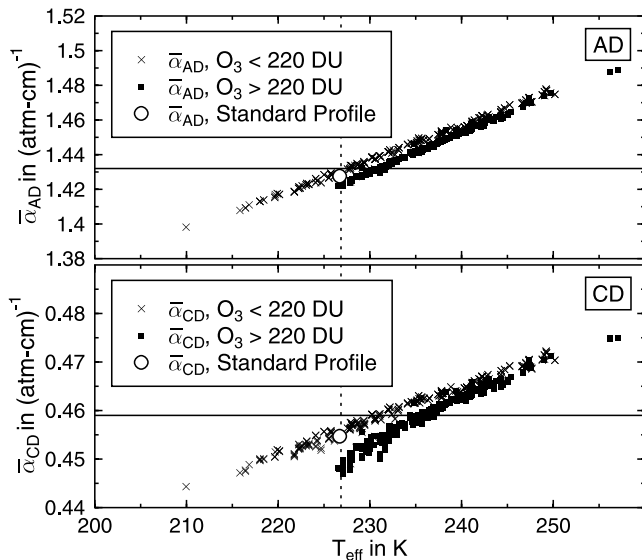


Figure 2. Effective ozone absorption coefficients $\bar{\alpha}_{AD}$ and $\bar{\alpha}_{CD}$, calculated from ozone profiles measured by Climate Monitoring and Diagnostics Laboratory (CMDL) at the South Pole, as a function of effective temperature T_{eff} . Data are divided into subsets with total column O_3 below and above 220 Dobson units (DU) (1 DU = 0.001 atm cm). The vertical dashed line indicates the standard temperature of -46.3°C . Solid lines indicate the values $\bar{\alpha}_{AD}^{\text{adjusted}} = 1.432$ and $\bar{\alpha}_{CD}^{\text{adjusted}} = 0.459$. Circles indicate our calculations of (top) $\bar{\alpha}_{AD}$ and (bottom) $\bar{\alpha}_{CD}$ for the standard conditions defined in Table 2.

tive ozone absorption coefficient $\bar{\alpha}_i$, $\bar{\alpha}_i^{\text{approx}}$, and $\bar{\alpha}_i^{\text{adjusted}}$, calculated by K93 and us. Values of the various coefficients are also provided in Table 1.

[18] Our values of $\bar{\alpha}_i^{\text{approx}}$ agree with the corresponding values of K93 to within $\pm 1.2\%$. A similar comparison for $\bar{\alpha}_i$ indicates agreement to within $\pm 2.3\%$, except for $\bar{\alpha}_{339.9}$ where our value is 0.010 and the value of K93 is 0.017 (67% difference). Figure 1a indicates that the value of K93 is unreasonably high, as it is close to the maximum of $\alpha(\lambda)$ in the wavelength interval defined by the Dobson slit function $S(\lambda, \lambda_{339.9})$. There is also no explanation for the large difference of 63% between $\bar{\alpha}_{339.9}$ and $\bar{\alpha}_{339.9}^{\text{approx}}$ in the K93 data set (Table 1). Additional calculations using the *Burrows et al.* [1999] O_3 CS showed that our extension of the *Bass and Paur* [1985] O_3 CS with the *Molina and Molina* [1986] O_3 CS above 340 nm cannot be the reason for the discrepancy. We therefore conclude that the value of $\bar{\alpha}_{339.9}$ given by K93 is unreasonably high. The difference in $\bar{\alpha}_{339.9}$ leads to differences of 1.9%, 1.5% and 0.5% in $\bar{\alpha}_D$, $\bar{\alpha}_{CD}$, and $\bar{\alpha}_{AD}$, respectively.

[19] The empirically adjusted value $\bar{\alpha}_D^{\text{adjusted}}$ agrees with our calculation of $\bar{\alpha}_D$ better than the unadjusted value. This indicates that most of the bias in $\bar{\alpha}_D$ caused by the error in $\bar{\alpha}_{339.9}$ was removed by the adjustment, and the coefficients $\bar{\alpha}_D$, $\bar{\alpha}_{CD}$, and $\bar{\alpha}_{AD}$ currently implemented by WMO should therefore be accurate to within $\pm 1\%$.

[20] Note that our and K93's value for $\bar{\alpha}_B$ agree to within 0.2%, whereas $\bar{\alpha}_B^{\text{adjusted}}$ is high by 1.1%. This suggests that the modification of $\bar{\alpha}_B$ by K93 may have been inappropriate. Calculations of effective Rayleigh scattering coeffi-

cients $\bar{\beta}_i$ by K93 and us agree to within $\pm 0.3\%$ at all wavelengths.

4. Effect of Approximations in Standard Dobson Data Reduction Method

4.1. Effective Ozone Absorption Coefficient

[21] The standard Dobson data reduction method (denoted as SM hereinafter) [*Basher*, 1982] applies the set of adjusted ozone absorption coefficients $\bar{\alpha}_i^{\text{adjusted}}$ to Dobson measurements from all stations. This may lead to systematic errors since $\sigma(\lambda, T)$ is temperature-dependent and actual atmospheric temperatures and their vertical distribution may differ from the standard value of -46.3°C . The error was quantified by calculating $\bar{\alpha}_i$ with equation (7) for direct Sun measurements of Dobson numbers 80 and 82 performed at the South Pole between 1991 and 2003. Both instruments have been repeatedly calibrated against the reference Dobson instrument number 83, which is, in turn, regularly calibrated with the Langley method at the Mauna Loa Observatory, Hawaii (20°N , 156°E , 3397 m above sea level). This cross-calibration procedure has been described by *Komhyr et al.* [1989] and calibration records for instrument numbers 80 and 82 were published in CMDL summary reports, for example [*CMDL*, 2002]. For the calculation of $\bar{\alpha}_i$, ozone and temperature profiles as well as surface pressure were taken from ozonesonde observations performed by CMDL at the South Pole. Balloons were launched approximately every third day during the austral spring [*Hofmann et al.*, 1997]. Only profiles with a burst altitude of at least 30 km were used, and profiles were extrapolated to higher altitudes using an algorithm described by *Bernhard et al.* [2002]. Other parameters were identical with those given in Table 1. Figure 2 shows $\bar{\alpha}_{AD}$ and $\bar{\alpha}_{CD}$ as a function of effective temperature T_{eff} (or ozone-weighted mean temperature), defined as

$$T_{\text{eff}} = \frac{\int_{z_0}^{\infty} T(z)\rho(z)dz}{\int_{z_0}^{\infty} \rho(z)dz}. \quad (12)$$

Both coefficients $\bar{\alpha}_{AD}$ and $\bar{\alpha}_{CD}$ increase with T_{eff} , but there is also some dependence on ozone column X : For the same T_{eff} , absorption coefficients are generally smaller when $X > 220$ DU than when $X < 220$ DU (i.e., “ozone hole” condition). Larger ozone abundance shifts the solar spectrum to longer wavelengths where $\alpha(\lambda)$ is smaller, leading to smaller values for $\bar{\alpha}_{AD}$ and $\bar{\alpha}_{CD}$. For a similar reason, $\bar{\alpha}_{AD}$ and $\bar{\alpha}_{CD}$ are smaller at larger air mass. Figure 3 shows a time series of T_{eff} at the South Pole.

[22] Figure 4 depicts the ratios of $\bar{\alpha}_{AD}$ and $\bar{\alpha}_{CD}$, calculated with the method described above, to associated standard values of 1.432 and 0.459 used by SM. Calculated values deviate from standard values by up to $\pm 4\%$. According to equation (3), underestimating $\bar{\alpha}_{AD}$ or $\bar{\alpha}_{CD}$ by 4% leads to an overestimate of X by 4%.

4.2. Relative Optical Air Mass Corresponding to Ozone Absorption

[23] In SM, μ is calculated with equation (11). This is an approximation since the actual ozone layer is not a delta

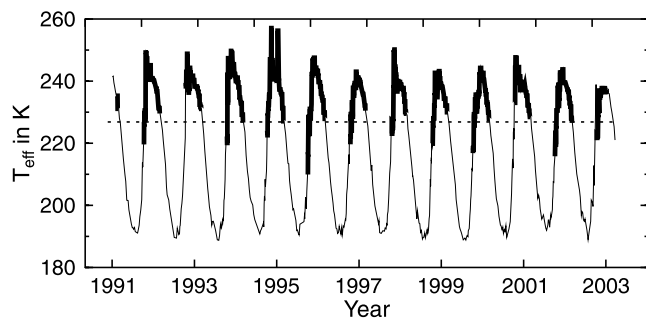


Figure 3. Effective temperature T_{eff} at the South Pole calculated from ozone profiles measured by CMDL. The thick line indicates periods when Dobson measurements are available. The dashed line indicates the standard temperature of -46.3°C .

layer at a fixed height h . Furthermore, the dependence of the index of refraction on altitude is neglected, and the true SZA, θ , rather than the apparent SZA, θ_0 , is typically used for calculations. For measurements at the South Pole, the following values for R , r , and h are implemented: $R = 6356.912$ km, $r = 2.81$ km, and $h = 17$ km. To quantify the effect of these approximations, we calculated air mass with equation (9) for all Dobson observations between February 1991 and January 2003 using the real atmospheric conditions taken from CMDL balloon profiles measured closest in time to the Dobson observations. The refraction index n of air and its dependence on pressure and temperature was calculated with the parameterization suggested by Edlén [1966] for a wavelength of $\lambda = 310$ nm. The apparent SZA, θ_0 , was calculated from θ as suggested by Thomason *et al.* [1983] by taking the actual pressure and temperature profiles into account. Figure 5 shows the difference $\theta - \theta_0$ of true and apparent SZA at the South Pole. Using the true rather than the apparent SZA for the calculation of μ will lead to an overestimate of μ . At $\theta = 85^{\circ}$, the overestimate is approximately 2%, which will, in turn, lead to an underestimate of 2% of the retrieved ozone column X .

[24] Figure 6 shows a comparison of the calculated air mass values using either the exact solution (equation (9)) or the approximation used in SM (equation (11)). Figure 6

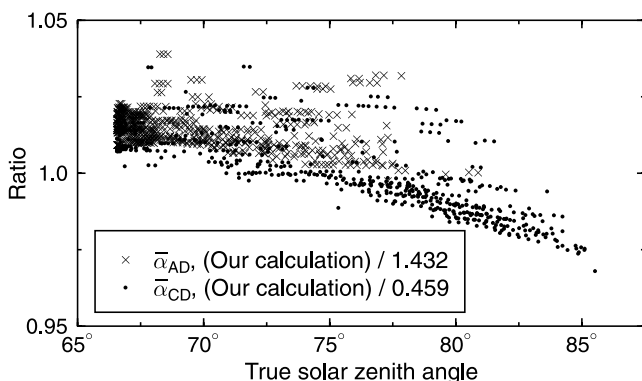


Figure 4. Ratio of effective ozone absorption coefficients $\bar{\alpha}_{\text{AD}}$ and $\bar{\alpha}_{\text{CD}}$, calculated from ozone profiles measured by CMDL at the South Pole, to associated standard values of 1.432 and 0.459, respectively.

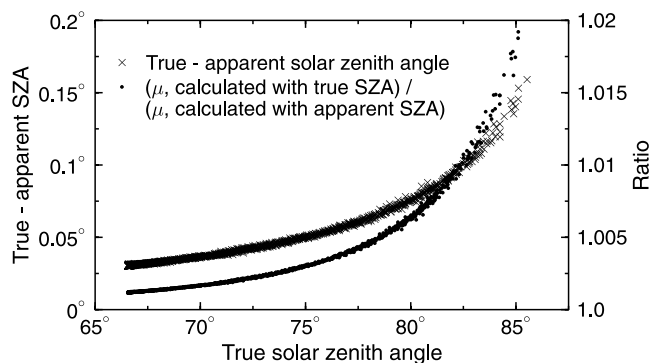


Figure 5. Effect of solar zenith angle type on air mass calculation. Difference of true and apparent solar zenith angle (crosses, left axis). Ratio of air mass calculated with true solar zenith angle to air mass calculated with apparent solar zenith angle (dots, right axis).

indicates that the actual air mass is lower by 1–4% than the approximated air mass. The difference increases with SZA and is largest for periods affected by the ozone hole.

[25] The total systematic error in total ozone column due to the approximations discussed above depends on the product $\mu\bar{\alpha}_{\text{AD}}$ for the Dobson AD pair and on $\mu\bar{\alpha}_{\text{CD}}$ for the Dobson CD pair. Figure 7 shows a comparison of $\mu\bar{\alpha}_{\text{AD}}$ and $\mu\bar{\alpha}_{\text{CD}}$ calculated either from the actual profiles or with SM. For SZAs smaller than 75° , calculations of the two products using the profile information are slightly larger than results obtained with SM. At larger SZA, the effect of the air mass becomes dominant and the sign of the difference reverses. At $\theta = 85^{\circ}$, SM overestimates $\mu\bar{\alpha}_{\text{CD}}$ by approximately 5%, leading to an underestimate of total ozone by about 5%.

5. Comparison With Other Total Ozone Data

[26] Dobson total ozone measurements from the period February 1991 and January 2003 were corrected by dividing the uncorrected data by the ratios shown in Figure 7. Uncorrected and corrected Dobson measurements were compared with total ozone data retrieved from UV spectra

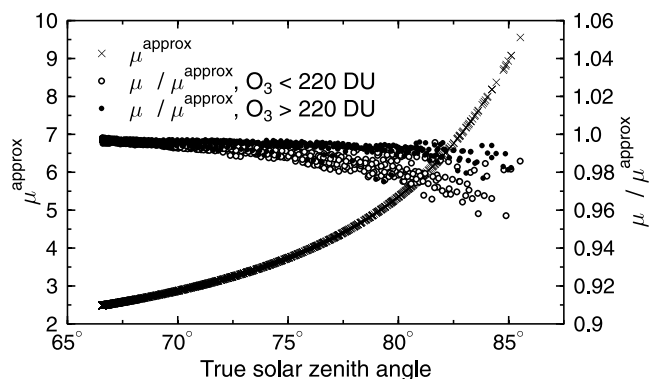


Figure 6. Comparison of relative optical air masses μ and μ^{approx} . Here μ was calculated with equation (9); μ^{approx} (crosses, left axis) was calculated with equation (11). Ratio μ/μ^{approx} for total ozone below 220 DU (open circles, right axis). Ratio μ/μ^{approx} for total ozone above 220 DU (solid circles, right axis).

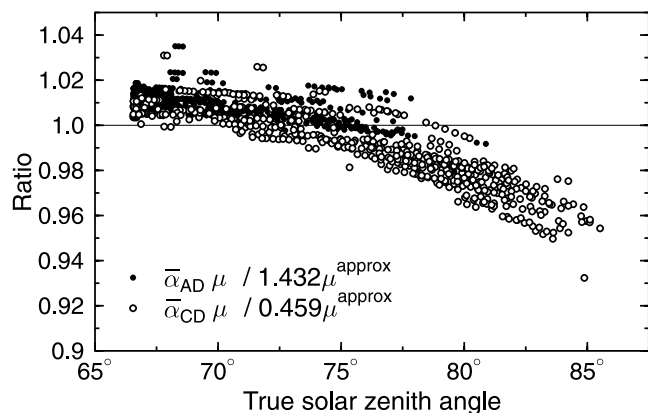


Figure 7. Comparison of product of ozone absorption coefficients and air mass, calculated either from ozone profiles measured by CMDL at the South Pole or with the standard Dobson method: ratio $\bar{\alpha}_{AD} \mu / 1.432 \mu^{\text{approx}}$ (solid circles) and ratio $\bar{\alpha}_{CD} \mu / 0.459 \mu^{\text{approx}}$ (open circles).

measured by a SUV-100 spectroradiometer at the South Pole. The instrument is part of the National Science Foundation's UV monitoring network, operated by Biospherical Instruments, Inc. [Booth *et al.*, 1994; Bernhard *et al.*, 2004]. It is located in the same building as the Dobson spectrophotometer. UV spectra are recorded every 15 min (60 min before 1997). The 2σ uncertainty of spectral irradiance at 310 nm measured by the instrument is 6.4% [Bernhard *et al.*, 2004]. Total ozone was calculated with an inversion method described by Bernhard *et al.* [2003]. In brief, the method compares SUV-100 spectra with several spectra that were calculated with the radiative transfer model UVSPEC/libRadtran [Mayer *et al.*, 1997] using different settings of the model total ozone value. The ozone value returned by the method is the model ozone value that leads to the best agreement between measurement and model. The CMDL ozone profiles used in sections 3 and 4 for the calculation of

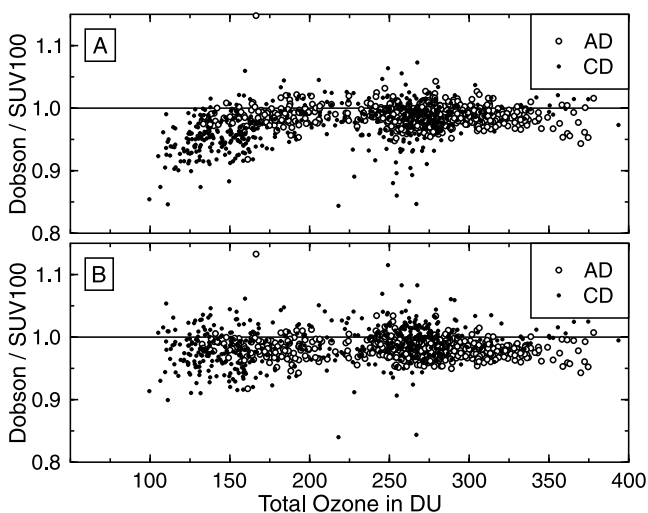


Figure 8. (a) Ratio of uncorrected (i.e., original) Dobson total ozone data and SUV-100 data at the South Pole. (b) Ratio of corrected Dobson total ozone data and SUV-100 data.

$\bar{\alpha}_i$ and μ were also used in UVSPEC model calculation. Thus the temperature-dependent vertical ozone distribution is also considered in the SUV-100 data set. The Barnes and Mauersberger [1987] correction (equation (6)) was not implemented. It can therefore be expected that SUV-100 data are too high by approximately 0.6%.

[27] Figure 8a depicts the ratio of uncorrected Dobson data to SUV-100 data. The ratio shows some dependence on total ozone: There is generally good agreement for total ozone values larger than 170 DU. When total ozone is below 170 DU, Dobson measurements are low by 4% on average. Figure 8b shows a similar ratio using the corrected Dobson data set. The dependence on total ozone is mostly absent in the corrected ratio. Dobson data are on average lower by 1.6% than SUV-100 data.

[28] Figure 9 presents a comparison of the SUV-100 data set with Version 8 overpass data from NASA's Total Ozone Mapping Spectrometer (TOMS) deployed on Nimbus 7 (1978–1993) and Earth Probe (1996 to present) satellites. TOMS data are on average 1.7% lower than SUV-100 data. This difference is still within the 2σ uncertainty of SUV-100 ozone data, which is $\pm 2.5\%$ for $\text{SZA} < 75^\circ$ and $\pm 4\%$ for $\text{SZA} > 75^\circ$ [Bernhard *et al.*, 2003]. The ratio of the two data sets depends only slightly on total ozone.

[29] Version 8 TOMS data are based on an improved retrieval algorithm, featuring a more accurate a priori ozone profile climatology derived from ozonesondes below 25 km, and Stratospheric Aerosol and Gas Experiment (SAGE) and Microwave Limb Sounder (MLS) measurements above 25 km. The data is averaged into monthly 10° latitude bins with an altitude resolution of approximately 1 km. For the polar vortex region (80° – 90°S), over 18,000 individual MLS measurements were averaged as well as over 900 ozonesondes, which were launched from the South Pole Station from 1988 to 2003. Analysis shows that if an ozone profile were perturbed by 10% in the 20–40 km region, TOMS ozone values would have an error of less than 1% at slant column density (μX) of less than 1500 DU, and 3.5% at a slant column of 3000 DU. The Version 8 temperature profile climatology has been created from National Centers for Environmental Prediction (NCEP) data and gridded to monthly 10° latitude bins with an altitude resolution of approximately 5 km. The TOMS Version 8 algorithm further includes an improved cloud height database from the Nimbus 7 Temperature Humidity Infrared Radiometer (NIMBUS-7 THIR); a better snow/ice climatology; a more accurate terrain height database; and additional aerosol and

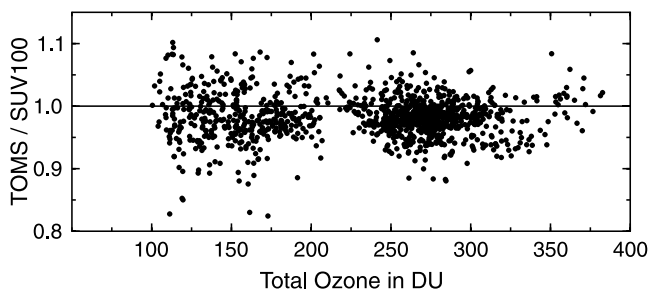


Figure 9. Ratio of Total Ozone Mapping Spectrometer (TOMS) Version 8 and SUV-100 total ozone data at the South Pole.

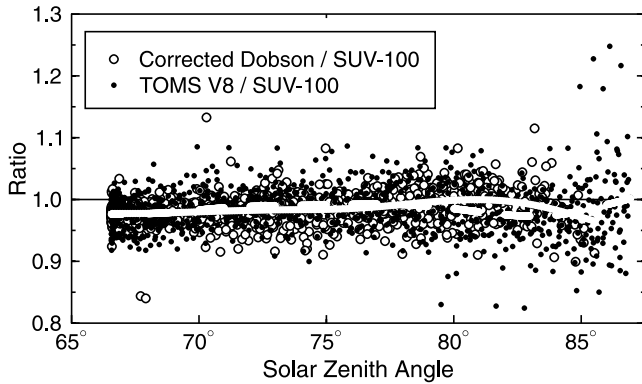


Figure 10. Comparison of corrected Dobson and TOMS data sets with SUV-100 ozone observations as a function of solar zenith angle: Ratio of corrected Dobson total ozone data to SUV-100 ozone (open circles) and ratio of TOMS Version 8 to SUV-100 data (solid circles). The solid white line is a smoothed fit to the ratio Dobson/SUV-100. The dashed white line is a smoothed fit to the ratio TOMS/SUV-100.

sea glint corrections [Labow et al., 2004; Wellemeyer et al., 2004]. A comparison of Earth Probe TOMS Version 8 total ozone data with data from 87 ground stations (Dobson and Brewer instruments) indicates that the average bias between the satellite and the ensemble of ground stations is smaller than $\pm 3\%$ and largely independent of latitude [Labow et al., 2004]. A comprehensive uncertainty budget for TOMS Version 8 data is still outstanding.

[30] Figure 10 presents a comparison of the Dobson and TOMS data sets with SUV-100 ozone observations as a function of SZA. We chose SUV-100 data as the common reference since SUV-100 spectra are measured close in time with both Dobson observations and the TOMS overpass. Trend lines were fitted to the data to facilitate the comparison. These trend lines indicate that corrected Dobson data and TOMS data agree on average to within 1% for SZA up to 80° . Above 80° , Dobson data tend to be larger by 1–2%. Uncorrected Dobson data are clearly lower than SUV-100 and TOMS data for SZAs larger than 83° . TOMS data are less than SUV-100 data by 1.7% on average, almost independent of SZA. Statistics of the comparison are provided in Table 3.

6. Conclusions

[31] A new set of ozone absorption coefficients $\bar{\alpha}_i$ for Dobson spectrophotometers was calculated and compared with results of similar calculation by K93, which form the basis of the coefficients recommend by WMO [Hudson et al., 1991]. K93’s and our coefficients agree to within $\pm 2.3\%$ for all but the Dobson wavelength at 339.9 nm. Some of the differences may be explained by the slightly different parameters used by K93 and us (Table 2). Our calculations use the most up-to-date data for the extraterrestrial spectrum and Rayleigh optical depth. Differences in slit function parameterization by K93 and us can lead to variations in $\bar{\alpha}_i$ due to the large change of ozone absorption within the band pass of the Dobson instrument. However, variations in center wavelengths and band pass of individual Dobson

spectrophotometers deployed worldwide are likely larger than the difference in slit function data implemented by K93 and us. Unfortunately, only the slit functions of the Standard Dobson number 83 have been measured with a tunable light source (K93). Slit functions of other Dobson photometers are assumed to be similar and only wavelength calibration and band pass are routinely (e.g., monthly) checked with mercury discharge lamps [Komhyr, 1980b].

[32] The value for $\bar{\alpha}_{339.9}$ is 0.017 in K93’s calculation and 0.010 in ours. Our analysis indicates that the value of 0.017 is unreasonably large and likely caused by an error in K93’s calculations. The difference of 67% between the two values leads to differences of 1.9%, 1.5% and 0.5% in $\bar{\alpha}_D$, $\bar{\alpha}_{CD}$, and $\bar{\alpha}_{AD}$, respectively. The value for $\bar{\alpha}_D$ currently recommended by WMO is K93’s $\bar{\alpha}_D$ value, but increased by 2.0%. Our analysis provides evidence that this empirical modification was justified. Differences between the WMO values and our calculations are -0.8% , 0.3% and 0.9% for $\bar{\alpha}_D$, $\bar{\alpha}_{AD}$, and $\bar{\alpha}_{CD}$, respectively.

[33] We found no clear justification for the empirical increase of $\bar{\alpha}_B$ by 1.3% suggested by K93 and implemented by WMO. This is of little consequence since the B-wavelength pair is rarely used for total ozone determination.

[34] The standard Dobson method assumes a constant stratospheric temperature of -46.3°C . It does not account for actual temperature variations, which affect ozone absorption via the temperature dependence of the O_3CS . At the South Pole, effective temperatures vary between -50°C and -18°C during the summer season (Figure 3). Temperatures often exceeded -46.3°C , which causes an underestimate of the effective ozone absorption coefficients (Figure 4), and an overestimate of the resulting total ozone values.

[35] The simplification that the ozone layer is confined to a delta layer at 17 km leads to an overestimate of the relative ozone air mass (Figure 6), which, in turn, leads to an underestimate of ozone. This systematic error increases with SZA and is largest when the ozone profile is distorted by the “ozone hole.” Using the true rather than the apparent SZA for the calculation of air mass further increases the error in μ .

Table 3. Statistics of Comparison of SUV-100, Dobson, and TOMS Total Ozone Data at South Pole

Data Set	Ratio $\pm 1\sigma$
<i>Dobson Uncorrected/SUV-100</i>	
All data	0.980 \pm 0.027
SZA < 80°	0.984 \pm 0.025
Dobson AD pair	0.988 \pm 0.016
Dobson CD pair, ozone > 220 DU	0.983 \pm 0.030
Dobson CD pair, ozone < 220 DU	0.959 \pm 0.033
<i>Dobson Corrected/SUV-100</i>	
All data	0.984 \pm 0.024
SZA < 80°	0.982 \pm 0.022
Dobson AD pair	0.980 \pm 0.015
Dobson CD pair, ozone > 220 DU	0.997 \pm 0.028
Dobson CD pair, ozone < 220 DU	0.979 \pm 0.032
<i>TOMS Version 8/SUV-100</i>	
All data	0.983 \pm 0.038
SZA < 80°	0.984 \pm 0.029
Nimbus 7 (Feb. 1991 to March 1993)	0.992 \pm 0.035
Earth Probe (Oct. 1996 to Jan. 2003)	0.980 \pm 0.038

[36] Comparisons with total ozone data from a SUV-100 spectroradiometer located at the South Pole and TOMS Version 8 data indicate that the uncorrected Dobson data set is too low at small ozone columns and/or large SZAs. In contrast, a comparison of the corrected Dobson data set with SUV-100 and TOMS measurements exhibit no clear dependence on total ozone or SZA. This indicates that the corrections applied to the Dobson data set lead to an overall accuracy improvement. Corrected Dobson data agree with TOMS to within $\pm 0.5\%$ on average. Corrected Dobson measurements are on average lower than SUV-100 measurements by 1.6%. 0.6% of this difference can be explained by the omission of the *Barnes and Mauersberger* [1987] correction in the SUV-100 data set. The remaining difference is still unresolved, but lies within the uncertainty of the SUV-100 ozone retrieval method [Bernhard et al., 2003] and the uncertainty of Dobson measurements [Komhyr, 1980a; Basher, 1982; Josefsson, 1992; Nichol and Valenti, 1993].

[37] It should be noted that corrections applied to Dobson data are smaller than $\pm 2\%$ for $SZA < 77^\circ$ ($\mu < 4.25$). The majority of Dobson observations performed worldwide is made at smaller SZAs. Systematic errors discussed in this paper are therefore relevant mostly for high-latitude sites where observations at small SZAs are not possible. However, low-latitude sites may also be affected by significant errors when stratospheric temperatures deviate substantially from -46.3°C .

[38] **Acknowledgments.** We acknowledge Bryan Johnson from CMDL for his help with the ozonesondes data. We especially appreciate the invaluable efforts of the many CMDL technical staff members and NOAA Corps Officers who operate the facility year-round at the South Pole to obtain the data used in this report. The U.S. National Science Foundation's Office of Polar Programs (NSF/OPP) supplied the logistics support for the facility at the South Pole. SUV-100 measurements at the South Pole were supported by NSF/OPP via a subcontract to Biospherical Instruments, Inc. from Raytheon Polar Services Company. The new TOMS Version 8 ozone retrieval was created and implemented by the Ozone Processing Team at NASA Goddard Space Flight Center, particularly P. K. Bhartia, R. D. McPeters, and C. Wellemeier.

References

- Anderson, G. P., S. A. Clough, F. X. Kneizys, J. H. Chetwynd, and E. O. Shettle (1986), AFGL atmospheric constituents profiles (0–120 km), *Tech. Rep. AFGL-TR-86-0110*, Air Force Geophys. Lab., Bedford, Mass.
- Barnes, J., and K. Mauersberger (1987), Temperature dependence of the ozone absorption cross section at the 253.7-nm mercury line, *J. Geophys. Res.*, *92*(D12), 14,861–14,864.
- Basher, R. E. (1982), Review of the Dobson spectrophotometer and its accuracy, *WMO Global Ozone Res. Monit. Proj. Rep. 13*, World Meteorol. Organ., Geneva, Switzerland.
- Bass, A. M., and R. J. Paur (1985), The ultraviolet cross-sections of ozone: 1. The measurements, in *Atmospheric Ozone*, edited by C. Zerefos and A. Ghazi, pp. 606–616, Springer, New York.
- Bates, D. R. (1984), Rayleigh scattering in air, *Planet. Space Sci.*, *32*(6), 785–790.
- Bernhard, G., C. R. Booth, and J. C. Ehranjian (2002), Comparison of measured and modeled spectral ultraviolet irradiance at Antarctic stations used to determine biases in total ozone data from various sources, in *Ultraviolet Ground- and Space-based Measurements, Models, and Effects*, edited by J. R. Slusser, J. R. Herman, and W. Gao, *Proc. SPIE Int. Soc. Opt. Eng.*, *4482*, 115–126.
- Bernhard, G., C. R. Booth, and R. D. McPeters (2003), Calculation of total column ozone from global UV spectra at high latitudes, *J. Geophys. Res.*, *108*(D17), 4532, doi:10.1029/2003JD003450.
- Bernhard, G., C. R. Booth, and J. C. Ehranjian (2004), Version 2 data of the National Science Foundation's Ultraviolet Radiation Monitoring Network: South Pole, *J. Geophys. Res.*, *109*, D21207, doi:10.1029/2004JD004937.
- Bodhaine, B. A., N. B. Wood, E. G. Dutton, and J. R. Slusser (1999), On Rayleigh optical depth calculations, *J. Atmos. Oceanic Tech.*, *16*, 1854–1861.
- Booth, C. R., T. B. Lucas, J. H. Morrow, C. S. Weiler, and P. A. Penhale (1994), The United States National Science Foundation's polar network for monitoring ultraviolet radiation, in *Ultraviolet Radiation in Antarctica: Measurements and Biological Effects*, *Antarct. Res. Ser.*, vol. 62, edited by C. S. Weiler and P. A. Penhale, pp. 17–37, AGU, Washington, D. C.
- Bhartia, P. K., D. Silberstein, B. Monosmith, and A. J. Fleig (1985), Standard profiles of ozone from ground to 60 km obtained by combining satellites and ground based measurements, in *Atmospheric Ozone: Proceeding of the Quadrennial Ozone Symposium Held in Halkidiki, Greece, 3–7 September 1984*, edited by C. S. Zerefos and A. Ghazi, pp. 243–247, Springer, New York.
- Brinksmas, E. J., et al. (2000), Validation of 3 years of ozone measurements over Network for the Detection of Stratospheric Change station Lauder, New Zealand, *J. Geophys. Res.*, *105*(D13), 17,291–17,306.
- Burrows, J. P., A. Dehn, B. Deters, S. Himmelmann, A. Richter, S. Voigt, and J. Orphal (1999), Atmospheric remote-sensing reference data from GOME: 2. Temperature-dependent absorption cross sections of O_3 in the 231–794 nm range, *J. Quant. Spectrosc. Radiat. Transfer*, *61*, 509–517.
- Climate Monitoring and Diagnostics Laboratory (2002), Climate Monitoring and Diagnostics Laboratory summary report no. 26 2000–2001, edited by D. B. King et al., U.S. Dep. of Comm., Boulder, Colo.
- Climate Monitoring and Diagnostics Laboratory (2004), Climate Monitoring and Diagnostics Laboratory summary report no. 27 2002–2003, edited by R. C. Schnell, A.-M. Buggle, and R. M. Rosson, U.S. Dep. of Comm., Boulder, Colo.
- Dobson, G. M. B. (1931), A photoelectric spectrophotometer for measuring the amount of atmospheric ozone, *Proc. Phys. Soc. London*, *43*, 324–337.
- Dobson, G. M. B., and D. N. Harrison (1926), Measurements of the amount of ozone in the Earth's atmosphere and its relation to other geophysical conditions, *Proc. R. Soc. London, Ser. A*, *110*, 660–693.
- Edlén, B. (1966), The refractive index of air, *Metrologia*, *2*, 71–80.
- Furukawa, P. M., P. L. Haagenson, and M. J. Scharberg (1967), A composite high-resolution solar spectrum from 2080 to 3600 Å, *NCAR TN-26*, 55 pp., Natl. Cent. for Atmos. Res., Boulder, Colo.
- Gueymard, C. A. (2004), The Sun's total and spectral irradiance for solar energy applications and solar radiation models, *Sol. Energy*, *76*(4), 423–453.
- Hofmann, D. J., S. J. Oltmans, J. M. Harris, B. J. Johnson, and J. A. Lathrop (1997), Ten years of ozonesonde measurements at the South Pole: Implications for recovery of springtime Antarctic ozone, *J. Geophys. Res.*, *102*(D7), 8931–8943.
- Hudson, R. D., W. D. Komhyr, C. L. Mateer, and R. D. Bojkov (1991), Guidance for use of new ozone absorption coefficients in processing Dobson and Brewer spectro-photometer total ozone data beginning 1 January, 1992, *WMO Doc. RDP-825*, World Meteorol. Organ., Geneva, Switzerland.
- Josefsson, W. A. P. (1992), Focused Sun observations using a Brewer ozone spectrophotometer, *J. Geophys. Res.*, *97*(D14), 15,813–15,817.
- Komhyr, W. D. (1980a), Dobson spectrophotometer systematic total ozone measurement error, *Geophys. Res. Lett.*, *7*(2), 161–163.
- Komhyr, W. D. (1980b), Operations handbook—Ozone observations with a Dobson spectrophotometer, *WMO Global Ozone Res. Monit. Proj. Rep. 6*, 125 pp., World Meteorol. Organ., Geneva, Switzerland.
- Komhyr, W. D., R. D. Grass, and R. K. Leonard (1989), Dobson spectrophotometer 83: A standard for total ozone measurements, 1962–1987, *J. Geophys. Res.*, *94*(D7), 9847–9861.
- Komhyr, W. D., C. L. Mateer, and R. D. Hudson (1993), Effective Bass-Paur 1985 ozone absorption coefficients for use with Dobson ozone spectrophotometers, *J. Geophys. Res.*, *98*(D11), 20,451–20,465.
- Kurucz, R. L., I. Furenlid, J. Brault, and L. Testerman (1984), Solar flux atlas from 296 to 1300 nm, technical report, 240 pp., Natl. Sol. Obs., Sunspot, N. M.
- Labow, G. J., R. D. McPeters, and P. K. Bhartia (2004), A comparison of TOMS and SBUV Version 8 total column ozone data with data from ground stations, in *Ozone, Proceedings of the XX Quadrennial Ozone Symposium, 1–8 June 2004, Kos, Greece*, vol. 1, edited by C. S. Zerefos, pp. 123–124, Int. Ozone Comm., Athens.
- Mayer, B., G. Seckmeyer, and A. Kylling (1997), Systematic long-term comparison of spectral UV measurements and UVSPEC modeling results, *J. Geophys. Res.*, *102*(D7), 8755–8768.
- Molina, L. T., and M. J. Molina (1986), Absolute absorption cross sections of ozone in the 185- to 350-nm wavelength range, *J. Geophys. Res.*, *91*(D13), 14,501–14,508.
- Nichol, S. E., and C. Valenti (1993), Intercomparison of total ozone measured at low Sun angles by the Brewer and Dobson spectrophotometers at Scott Base, Antarctica, *Geophys. Res. Lett.*, *20*(19), 2051–2054.

- Orphal, J. (2003), A critical review of the absorption cross-sections of O₃ and NO₂ in the ultraviolet and visible, *J. Photochem. Photobiol. A*, 157, 185–209.
- Thomason, L. W., B. M. Herman, and J. A. Reagan (1983), The effect of atmospheric attenuators with structured vertical distributions on air mass determinations and Langley plot analyses, *J. Atmos. Sci.*, 40, 1851–1854.
- Van Roozendaal, M., et al. (1998), Validation of ground-based visible measurements of total ozone by comparison with Dobson and Brewer spectrophotometers, *J. Atmos. Chem.*, 29(1), 55–83.
- Wellemeyer, C. G., P. K. Bhartia, R. D. McPeters, S. L. Taylor, and C. Ahn (2004), A new release of data from the Total Ozone Mapping Spectrometer (TOMS), *SPARC Newsl.* 22, 37–38. (Available at http://www.atmosp.physics.utoronto.ca/SPARC/News22/22_Wellemeyer.html)
-
- G. Bernhard, Biospherical Instruments Inc., 5340 Riley Street, San Diego, CA 92110, USA. (bernhard@biospherical.com)
- R. D. Evans and S. J. Oltmans, NOAA Climate Monitoring and Diagnostics Laboratory, 325 Broadway, Boulder, CO 80303, USA. (robert.d.evans@noaa.gov; samuel.j.oltmans@noaa.gov)
- G. J. Labow, NASA Goddard Space Flight Center, Greenbelt, MD 20771, USA. (labow@qhearts.gsfc.nasa.gov)